Molecular Pharmacology Fast Forward. Published on August 1, 2013 as doi:10.1124/mol.113.087072
This article has not been copyedited and formatted. The final version may differ from this version.

Mol Manuscript # 87072

Fluorescence correlation spectroscopy analysis of serotonin, adrenergic, muscarinic, and dopamine receptor dimerization: the oligomer number puzzle.

Katharine Herrick-Davis, Ellinor Grinde, Ann Cowan and Joseph E. Mazurkiewicz

Center for Neuropharmacology & Neuroscience,
Albany Medical College, Albany, NY 12208
KHD, EG, JEM

Center for Cell Analysis and Modeling,
University of Connecticut Health Center,
Farmington, CT 06030
AC

Molecular Pharmacology Fast Forward. Published on August 1, 2013 as DOI: 10.1124/mol.113.087072
This article has not been copyedited and formatted. The final version may differ from this version.

Mol Manuscript # 87072

Running title: FCS analysis of biogenic amine GPCR

Address correspondence to:
Katharine Herrick-Davis, Ph.D.
Professor
Center for Neuropharmacology & Neuroscience
Mail code - 136
Albany Medical College
47 New Scotland Ave.
Albany, NY 12208
daviskh@mail.amc.edu
tel 518-262-6357
fax 518-262-5799

Number of pages: 18

Number of tables: 2

Number of figures: 7

Number of references: 59

Number of words in Abstract: 250

Number of words in Introduction: 731

Number of words in Discussion: 1468
Non-standard abbreviations: FCS (fluorescence correlation spectroscopy); PCH (photon counting histogram); BiFC (bimolecular fluorescence complementation).

Molecular Pharmacology Fast Forward. Published on August 1, 2013 as DOI: 10.1124/mol.113.087072
This article has not been copyedited and formatted. The final version may differ from this version.

Abstract

The issue of G-protein coupled receptor (GPCR) oligomer status has not been resolved. While many studies have provided evidence in favor of receptor-receptor interactions, there is no consensus as to the exact oligomer size of class A GPCR. Previous studies have reported monomers, dimers, tetramers and higher order oligomers. In the present study this issue was examined using fluorescence correlation spectroscopy (FCS) with photon counting histogram (PCH) analysis, a sensitive method for monitoring diffusion and oligomer size of plasma membrane proteins. Six different class A GPCR were selected from the serotonin (5-HT_{2A}), adrenergic (α_{1b}-AR and β_2-AR), muscarinic (M_1 and M_2), and dopamine (D_1) receptor families. Each GPCR was C-terminally labeled with GFP or YFP and expressed in HEK293 cells. FCS provided plasma membrane diffusion coefficients on the order of $7.5x10^{-9}$ cm^2/s. PCH molecular brightness analysis was used to determine GPCR oligomer size. Known monomeric (CD-86) and dimeric (CD-28) receptors with GFP and YFP tags were used as controls to determine the molecular brightness of monomers and dimers. PCH analysis of fluorescence-tagged GPCR revealed molecular brightness values that were twice the monomeric controls and similar to the dimeric controls. Reduced chi square analyses of the PCH data best fit a model for a homogeneous population of homodimers, without tetramers or higher order oligomers. The homodimer configuration was unaltered by agonist treatment and was stable over a 10-fold range of receptor expression level. The results of this study demonstrate that biogenic amine receptors freely diffusing within the plasma membrane are predominantly homodimers.

Molecular Pharmacology Fast Forward. Published on August 1, 2013 as DOI: 10.1124/mol.113.087072
This article has not been copyedited and formatted. The final version may differ from this version.

Introduction

G-Protein coupled receptors (GPCR) represent one of the largest families of plasma membrane-associated receptors. They are present on virtually every cell in the human body and regulate a wide variety of physiological responses to light, odorants, hormones, neurotransmitters, and therapeutic agents. Physiological processes regulated by GPCR activation and blockade have been studied for decades, but there is still great debate as to what constitutes the functional signaling unit: is it a monomer, dimer or higher order oligomer? While monomeric GPCR in reconstituted lipid vesicles can activate G-proteins (Whorton et.al., 2007), GPCR dimers/oligomers have been reported in native tissues and primary cultures (Fotiadis et.al., 2003; Rashid et.al., 2007; Albizu et.al., 2010; Herrick-Davis et al., 2012; Knepp et.al., 2012; Teitler and Klein, 2012; Jastrzebska et.al., 2013). While the functional significance of class A GPCR dimerization is still a subject of great debate, GPCR homo- and hetero-dimerization have been reported to regulate ligand binding, second messenger activation and receptor trafficking (reviewed in Milligan, 2013).

For class A GPCR there is no consensus in the published literature as to their monomer/oligomer status. Quantitative studies designed to determine the monomeric/oligomeric composition of class A GPCR have reported the presence of monomers (James et.al., 2006; Meyer et.al., 2006; Dorsch et.al., 2009; Hern et.al., 2010; Kasai et.al., 2011), dimers (Mercier et.al., 2002; Canals et.al., 2004; Dorsch et.al., 2009; Goin and Nathanson, 2006; Harikumar et.al., 2008; Herrick-Davis et al., 2012; Knepp et.al., 2012; Teitler and Klein, 2012; Patowary et.al., 2013), tetramers (Fung et.al., 2009; Pisterzi et.al., 2010; Patowary et.al., 2013), and higher order oligomers (Guo et.al., 2008; Dorsch et.al., 2009; Albizu et.al., 2010; O'Dowd et.al., 2011). Co-immunoprecipitation (Co-IP), resonance energy transfer (RET), fluorescence lifetime imaging (FLIM), and bimolecular fluorescence complementation (BiFC) are commonly employed methods used to evaluate protein-protein interactions. However, immunoprecipitation requires solubilization and disruption of the native GPCR plasma membrane environment, and RET/BiFC are proximity-based assays that monitor the distance between the fluorescent probes. While these methods can provide evidence consistent with the hypothesis that GPCR form dimers/oligomers, they do not provide

Molecular Pharmacology Fast Forward. Published on August 1, 2013 as DOI: 10.1124/mol.113.087072
This article has not been copyedited and formatted. The final version may differ from this version.

conclusive proof of protein-protein interactions. Recently, purification of photo-activated rhodopsin from native disc membranes using lauryl-maltose-neopentyl-glycol and 3D projection analysis revealed a rhodopsin dimer in complex with a single G–protein (Jastrzebska et.al., 2013).

Fluorescence correlation spectroscopy (FCS) provides a good alternative for investigating diffusion and protein interactions in living cells. It requires very low protein expression levels, making it suitable for studying plasma membrane GPCR at physiological expression levels. FCS records the fluctuations in fluorescence intensity arising from individual fluorescent molecules, in a temporal manner (Magde et.al., 1972). Combining confocal microscopy with FCS led to the development of sensitive methods for monitoring protein dynamics in living cells (Qian and Elson, 1991; Rigler et.al.,1993; Pramanik et.al., 2001; Digman et.al., 2005). FCS has been used to monitor diffusion and ligand binding for ion channels, tyrosine kinase receptors and GPCR (reviewed in Briddon and Hill, 2007), to examine neuropeptide Y and beta-arrestin interactions (Kilpatrick et.al., 2012), and to monitor the oligomer status of various receptors including somatostatin (Patel et.al., 2002), epidermal growth factor (Liu et.al., 2007), ciliary neurotrophic factor (Neugart et.al., 2009), estrogen (Savatier et.al., 2010), and serotonin 5-HT1A (Ganguly and Chattopadhyay, 2010) and 5-HT_{2C} receptors (Herrick-Davis et.al., 2012).

The oligomer status of a protein cluster can be determined by analyzing the amplitude of the fluctuations in fluorescence intensity measured in an FCS experiment. A photon counting histogram (PCH) can be generated from the FCS data and used to determine the molecular brightness of a fluorescence-tagged protein (Chen et.al., 1999). Since the molecular brightness of a cluster of fluorescent molecules is directly proportional to the number of fluorescent molecules present in the cluster, the molecular brightness provides an estimate of the number of fluorescent molecules within the protein complex. Molecular brightness analysis has been used to explore the oligomeric status of nuclear retinoid X receptors (Chen et.al., 2003), epidermal growth factor receptors (Saffarian et.al., 2007), urokinase plasminogen activator receptors (Malengo et.L., 2008), and serotonin 5-HT_{2C} receptors (Herrick-Davis et.al., 2012).

Molecular Pharmacology Fast Forward. Published on August 1, 2013 as DOI: 10.1124/mol.113.087072
This article has not been copyedited and formatted. The final version may differ from this version.

FCS combined with confocal microscopy and PCH provide powerful methods for determining the molecular brightness of individual fluorescence-tagged proteins as a measure of their oligomer size. The present study describes the application of FCS and PCH analysis for determining the oligomeric size of biogenic amine serotonin (5-HT_{2A}), adrenergic (α_{1b}-AR and β_2-AR), muscarinic (M_1 and M_2), and dopamine (D_1) receptors freely diffusing within the plasma membrane of living cells.

Materials and Methods

Plasmids: cDNAs encoding the 5-HT_{2A}, α_{1b}-AR, β_2-AR, M_1-muscarinic, M_2-muscarinic, and D_1-dopamine receptors were PCR amplified from human total genomic DNA and cloned into the pEGFP-N1 and pEYFP-N1 vectors (Clonetech) at EcoRI/BamHI to create chimeric receptors with fluorescent tags on the C-terminus of the receptor. Site-directed mutagenesis (Stratagene) was used to create an A206K mutation in all GFP constructs and an L221K mutation in the monomeric YFP and dimeric CD-28/YFP constructs to eliminate potential aggregation of the fluorescent tags (Zacharias et.al., 2002). Bimolecular fluorescence complementation (BiFC) pairs, N-YFP and C-YFP, were made by site-directed mutagenesis using the β_2-AR/YFP cDNA as the starting template. β_2-AR/N-YFP was made by inserting a stop codon at amino acid 156 of YFP. β_2-AR/C-YFP was made by inserting a BamHI site at amino acid 156 of the YFP, followed by BamHI digest to remove amino acids 1-155 of the YFP, and subsequent re-ligation. The A_{2a}-adenosine BiFC constructs were a generously provided by S. Briddon. CD-28/YFP was a generous gift from J. Miller. CD-86/GFP and CD-86/GFP-GFP were generously provided by G. Milligan.

Cell culture, transfection and drug treatment: HEK293 cells (ATCC) were cultured in Dulbecco's Minimal Essential Medium (cellgro) with 10% FBS (HyClone) in a humidified chamber at 37^0C, 5% CO_2. HEK293 cells were plated in 6 well plates fitted with 25mm poly-D-lysine coated glass coverslips (Fisher) at a density of 5 x 10^5 cells per coverslip and transfected with 50ng of the indicated plasmid DNA using lipofectamine reagent (Invitrogen) for five hours. Following transfection, cells were cultured in MEM (without

Molecular Pharmacology Fast Forward. Published on August 1, 2013 as DOI: 10.1124/mol.113.087072
This article has not been copyedited and formatted. The final version may differ from this version.

phenol red) with 10% charcoal stripped serum (Gibco) for 20 hours at 37^0C, 5% CO_2. In our hands, this transfection protocol typically yields plasma membrane receptor expression levels on the order of one pmol/mg protein, by radioligand binding analysis. For drug treatment, isoproterenolol and carbachol were diluted in HEPES-buffered MEM (without phenol red) and added directly to the viewing chamber to achieve a final concentration of 0.1µM. FCS measurements were initiated 1 minute following the addition of ligand. We have previously determined this time point to be sufficient for receptor activation, measured as beta-arrestin recruitment to the plasma membrane (Herrick-Davis et.al., 2007, 2012).

Fluorescence correlation spectroscopy (FCS): For FCS measurements, cells were washed twice with HEPES-buffered Krebs-ringer (without glucose) and the coverslip was placed in a viewing chamber with 1ml of HEPES-buffered Minimal Essential Medium (MEM, without phenol red). FCS measurements were made using a Zeiss LSM-780 confocal microscope equipped with gallium arsenide phosphide (GaAsP) photon detectors (Carl Zeiss, Germany). One-photon excitation with a continuous argon ion laser was performed using a 40x (N.A. 1.2) C-apochromat water immersion objective to create an observation volume on the order of 10^{-15} liters. Since the observation volume is not illuminated homogenously, optimal positioning of the plasma membrane within the center of the observation volume is critical for accurate determination of the molecular brightness of fluorescent-tagged membrane proteins. FCS measurements were made on the apical plasma membrane, directly above the cell nucleus of HEK293 cells transfected with the indicated fluorescence-tagged receptor. Positioning of the plasma membrane in the center of the observation volume was achieved by monitoring the photon counts per molecule in real time (by opening the interactive counts/molecule window in the Zeiss software menu) while simultaneously focusing upward through the plasma membrane to identify the focal plane corresponding to the maximal photon counts per molecule. FCS measurements were recorded at 23^0C in HEPES-buffered MEM (without phenol red) for 100 seconds, as 10 consecutive 10 second intervals. As fluorescent-tagged receptors enter and diffuse through the observation volume they are excited by the laser. GFP and YFP were

Molecular Pharmacology Fast Forward. Published on August 1, 2013 as DOI: 10.1124/mol.113.087072
This article has not been copyedited and formatted. The final version may differ from this version.

excited at 488nm and 514nm, respectively, with a laser intensity of 0.1%. It is critical to use the lowest laser power possible, while still maintaining a good signal to noise ratio, as higher laser powers will result in photobleaching of the fluorescent probe. The time-dependent fluctuations in fluorescence intensity were recorded on GaAsP detectors as follows: emitted fluorescence captured by the objective is passed through an appropriate band pass filter and focused onto the detector using a pinhole of one airy unit. FCS recordings were analyzed by a digital temporal correlator (using non-linear least-squares minimization, Zeiss Aim 4.2 software) to calculate the autocorrelation function G(τ), which represents the time dependent decay in fluorescence fluctuation intensity as in equation 1a,

Equation 1a: $G(\tau) = \frac{<\delta F(t) \cdot \delta F(t+\tau)>}{<F(t)>^2}$

where G(τ) is the <time average> of the change in fluorescence fluctuation intensity (δF) at some time point (*t*) and at a time interval later (t + τ), divided by the square of the average fluorescence intensity. Autocorrelation analyses were performed using the Zeiss Aim 4.2 software package with an autocorrelation bin time of 0.2μs. FCS data were fit to a 2D model (for lateral diffusion within the plasma membrane) with 2 components as in equation 1b,

Equation 1b: $G(\tau) = 1 + AN^{-1}[F_1(1 + {}^{\tau}/_{\tau D1})^{-1} + F_2(1 + {}^{\tau}/_{\tau D2})^{-1}]$

where N is the number of molecules in the observation volume. F_1, F_2 and τD1, τD2 represent the respective fractions and diffusion times of the two components. A pre-exponential term is included to account for photophysical properties (blinking) of the fluorescent probe $\{A = 1 + \left(T_b e^{-\frac{\tau}{\tau b}}\right)(1 - T_b)^{-1}\}$ where T_b and τ_b represent the blinking fraction and relaxation time, respectively. It should be noted that individual GFP and YFP molecules are not always fluorescent. They can exhibit blinking, exist in a prolonged dark state, or be immature and non-fluorescent (Ulbrich and Isacoff, 2007)

Molecular Pharmacology Fast Forward. Published on August 1, 2013 as DOI: 10.1124/mol.113.087072
This article has not been copyedited and formatted. The final version may differ from this version.

The resulting autocorrelation curve depicts the fluorescence intensity fluctuations as a function of particle number and diffusion time. The average dwell time of the fluorescent species within the observation volume (τ_D) is calculated from the mid-point of the autocorrelation curve. The diffusion coefficient (*D*) for lateral diffusion of fluorescence-tagged GPCR within the plasma membrane can then be calculated as in equation 2, where ω_0 is the radial waist of the observation volume.

Equation 2: $$D = \frac{\omega_0^2}{4\tau_D}$$

The radial waist was determined experimentally from the full width at half maximum of a Gaussian distribution fitted to the image of sub-resolution fluorescent beads (FluoSpheres, 0.1um, Invitrogen) as described by Cole et al. 2010. In our experimental set-up, the radial waist was determined to be 0.30μm.

The amplitude of the autocorrelation function G(0) (equal to the y-intercept) is inversely related to the number of molecules in the observation volume (N_{PSF}) as in equation 3,

Equation 3: $$N_{PSF} = \frac{1}{G(0)-1} \cdot \gamma$$

where gamma is the point spread function (PSF) which describes the shape of the observation volume. The numerical value of gamma differs depending on the model selected for analysis and is 0.5 for 2D FCS analysis and 0.35 for a 3D Gaussian model used for PCH analysis. While the absolute numerical values of molecular brightness will vary depending on whether a 2D FCS or 3D PCH model is selected (due to the different numerical value of gamma used in equation 3) the overall conclusions will remain the same, as the molecular brightness of a dimer will still be twice that of a monomer regardless of the selected model.

The average fluorescence intensity or average photon count rate (k) recorded for a given sample is determined by the number of fluorescent molecules (N_{PSF}) and their molecular brightness (ε), as described in equation 4.

Molecular Pharmacology Fast Forward. Published on August 1, 2013 as DOI: 10.1124/mol.113.087072
This article has not been copyedited and formatted. The final version may differ from this version.

Equation 4: $k = N_{PSF} \cdot \varepsilon$

Thus dividing the count rate (k) by the number of molecules (N_{PSF}) provides an estimate of the molecular brightness (ε) of the sample.

Photon Counting Histogram (PCH): Fluorescence fluctuation data recorded during an FCS experiment can be used to generate photon counting histograms, which provide quantitative information about the number of fluorescent molecules and the number of photon counts per molecule (Chen et.al., 1999). PCH analysis uses a 3D Gaussian approximation of the laser beam profile. In the present study, cells transfected with fluorescence-tagged receptors were selected with an average plasma membrane photon count rate ranging from 50kHz to 250kHz, corresponding to plasma membrane receptor expression levels in the nanomolar range. Membrane regions containing ruffles, filopodia, and high concentrations of fluorescent proteins (>250kHz) were avoided. Ten measurements were made on the upper plasma membrane of each cell by monitoring the photon count rate for 100 seconds, as 10 consecutive 10 second observation periods. While the laser intensity was set to 0.1% to minimize photo-bleaching, photo-bleaching was apparent during the first 10 second observation period. Therefore, the average molecular brightness from the second through tenth observation periods was calculated and reported as the molecular brightness for that cell. Segments of the fluorescence intensity trace that showed large spikes or drifts in fluorescence intensity (due to cell movement) were excluded from the analysis. To generate a histogram, each 10 second observation period was broken down into one million intervals or bins (PCH bin time = 10μs). Histograms were constructed using the PCH module in the Zeiss Aim 4.2 software in which the number of 10μs bins was plotted on the y-axis and photon counts on the x-axis. The resulting histogram depicts the number of bins that registered 1,2,3 photon counts etc. during one 10 second observation period. Since a constant intensity light source produces a photon count distribution that follows Poisson statistics, as fluorescent molecules enter and diffuse through the non-homogenously illuminated observation volume, the fluctuations in fluorescence intensity

Molecular Pharmacology Fast Forward. Published on August 1, 2013 as DOI: 10.1124/mol.113.087072
This article has not been copyedited and formatted. The final version may differ from this version.

result in a broadening of the Poisson distribution. This super-Poisson characteristic is observed in the tail of PCH curve. Initially, PCH data were fit to a one component model where concentration and molecular brightness were allowed to be free (and the first order correction was fixed at zero) to determine the average molecular brightness of the sample.

Multi-component PCH analysis: The PCH data were subjected to a multi-component analysis to test for the presence of a mixture of monomers, dimers and tetramers. Fitting the PCH data to a multi-component model was performed as described by Müller and colleagues (Müller et al.,2000) using the PCH module in the Zeiss Aim4.2 analysis software. Molecular brightness values were fixed based on the control values for monomers and dimers obtained from the initial one component fit of the data (table 1). Reduced chi square analysis was used to determine the goodness of fit to both one component and multi-component models.

Controls for molecular brightness analysis: Five different plasma membrane controls were used to decode the molecular brightness of GFP- and YFP-tagged biogenic amine receptors. Known monomeric (CD-86) and dimeric (CD-28) plasma membrane receptors with C-terminal GFP (CD-86/GFP and CD-86/GFP-GFP) and YFP (CD-28/YFP) were used to determine the molecular brightness of GFP and YFP monomers and dimers. The β_2-AR/YFP BiFC pair and co-expression of β_2-AR/GFP or M_1/GFP with a three-fold excess of untagged, non-fluorescent receptor were used as additional controls. To eliminate self-aggregation of GFP or YFP (Zacharias et.al., 2002), all GFP constructs contained an A206K mutation and the CD-28/YFP construct contained an L221K mutation. To determine the contribution of background auto-fluorescence from cytoplasmic proteins, a dilute solution of purified monomeric GFP was evaluated. The molecular brightness of GFP in solution (8,268 CPSM) was similar to GFP from pEGFP plasmid expressed in the cytosol of HEK293 cells (8,508 CPSM), indicating that background auto-fluorescence from cytoplasmic proteins was minimal (approximately 3%) in our experimental set-up.

Molecular Pharmacology Fast Forward. Published on August 1, 2013 as DOI: 10.1124/mol.113.087072
This article has not been copyedited and formatted. The final version may differ from this version.

2D FCS analysis of molecular brightness with varying receptor expression levels: To investigate the relationship between molecular brightness and receptor expression level, 2D FCS analysis was used to determine the number of fluorescent molecules in the observation volume (as in equation 3) and the molecular brightness (as in equation 4). The area of plasma membrane in the observation volume was calculated using $\pi\omega_0^2$, where ω_0 is the radius of the observation volume (0.30μm), determined experimentally as described in equation 2. The total surface area of an HEK293 cell, determined to be 2591μm^2 (Sommerhage et.al., 2008), was used to estimate the total number of receptors per cell.

Results

Fluorescence correlation spectroscopy (FCS) and photon counting histogram (PCH) analyses were applied to determine the diffusion dynamics and oligomer status of biogenic amine GPCR selected from the serotonin (5-HT$_{2A}$), adrenergic (α_{1b}-AR and β_2-AR), muscarinic (M_1 and M_2), and dopamine (D_1) receptor families. Fluorescent probes (GFP or YFP) were attached to the C-terminus of each GPCR. In the present study, proper plasma membrane targeting of fluorescence-tagged GPCR was confirmed by confocal microscopy (figure 1). FCS measurements were made on the upper plasma membrane of transfected HEK293 cells (as shown in figure 1d).

In an FCS experiment, a high numerical aperture objective is used to focus a laser beam into a small diffraction-limited spot, creating a detection or observation volume on the order of 10^{-15} liters. The upper plasma membrane of HEK293 cells expressing fluorescence-tagged GPCR was positioned within the laser-illuminated observation volume by focusing upward from the middle of the cell to the top, while simultaneously monitoring the photon counts per molecule. Optimal positioning of the plasma membrane within the center of the observation volume is critical for accurate FCS/PCH analysis of molecular brightness as the detected photon counts decrease as fluorescent molecules travel away from the center of the observation volume. The fluorescence-tagged GPCR, freely diffusing within the plasma membrane, pass through the observation volume where they are excited by a laser and give off bursts of photons.

Molecular Pharmacology Fast Forward. Published on August 1, 2013 as DOI: 10.1124/mol.113.087072
This article has not been copyedited and formatted. The final version may differ from this version.

The fluctuations in fluorescence, produced by fluorescence-tagged GPCR entering and leaving the observation volume, are recorded in real time, as shown in the fluorescence intensity traces in figure 2a.

Autocorrelation analyses of the fluorescence intensity traces (from figure 2a) are performed using a non-linear least-squares fitting routine which graphically represents the autocorrelation function G(τ) on the ordinate and diffusion time on the abscissa (figure 2b). The rate at which GPCR diffuse within the plasma membrane is reported as the average dwell time (τ_D) of the fluorescence-tagged GPCR within the observation volume and is calculated from the mid-point of the autocorrelation decay curve. The biphasic autocorrelation curves shown in figure 2b are best fit by a two component model with a very fast component characteristic of the photo-physical properties of the fluorescent probe (τ_{D1}) and a slower component representing the translational diffusion of the GPCR within the plasma membrane (τ_{D2}).

Diffusion coefficients for fluorescence-tagged GPCR in HEK293 cell plasma membranes are reported in table 1. All diffusion data best fit a two-component model with τ_{D1} values related to the photo-physical properties of the fluorescent probe (50µs-100µs for YFP and 250µs-300µs for GFP) and τ_{D2} values (representing the average dwell time of the GPCR within the observation volume) on the order of 30ms, yielding a diffusion coefficient on the order of 7.5 x 10^{-9}cm^2/s. Since FCS measures the mobile fraction of freely diffusing proteins, fluorescence-tagged GPCR that are sequestered into microdomains with reduced mobility (Day and Kenworthy, 2009), or associated with cytoskeletal or extracellular matrix proteins, could photobleach during an FCS recording. In the present study, approximately 40-50% of the initial fluorescence signal was photobleached during the first 10 seconds of each FCS recording (data not shown). This phenomenon, observed for all six GPCR tested, is consistent with previous results obtained using fluorescence recovery after photobleach (FRAP) to monitor GPCR diffusion (Dorsch et.al., 2009; Fonesca and Lambert, 2011).

Figure 2 shows representative FCS autocorrelation graphs for YFP-tagged 5-HT_{2A}, β_2-AR, D_1-dopamine, M_2-muscarinic, dimeric CD-28 and the β_2-AR BiFC pair (β_2-AR/N-YFP + β_2-AR/C-YFP). Inspection of the fluorescence intensity traces in figure 2a

Molecular Pharmacology Fast Forward. Published on August 1, 2013 as DOI: 10.1124/mol.113.087072
This article has not been copyedited and formatted. The final version may differ from this version.

reveals similar average photon count rates for the GPCR and the dimeric CD-28/YFP control. The amplitude (y-intercept) of the autocorrelation curve (figure 2b) is inversely related to the number of fluorescent proteins or complexes present in the observation volume and was similar for the GPCR and CD-28/YFP. The molecular brightness of the YFP-tagged GPCR can be determined from the FCS data by dividing the average photon count rate obtained from the fluorescence intensity traces in figure 2a (130kHz on average for the GPCR and for the dimeric CD-28) by the number of fluorescent molecules calculated from the amplitude of the autocorrelation curves in figure 2b (using equation 3 in Methods with a 2D FCS model yields and average N=10). This provides an approximate molecular brightness of 13,000 counts per second per molecule (CPSM) for the GPCR and dimeric CD-28, consistent with a dimeric structure for the GPCR. The molecular brightness of the β_2-AR BiFC pair, estimated as 42 kHz (figure 2a) divided by 6.3 (the number of molecules determined from figure 2b using equation 3) is 6,667 CPSM, approximately half that of the YFP-tagged GPCR and dimeric CD-28.

PCH analysis uses a 3D Gaussian approximation of the laser beam profile and Poisson statistics to predict what the molecular brightness of the fluorescent particle would be when it is at the center of the observation volume (Chen et.al., 1999). Photon counting histograms were generated from the FCS data presented in figure 2. The shape of the histogram is a function of the number of fluorescent molecules and their molecular brightness, and was the same for the GPCR and dimeric CD-28 (figure 3). To generate a histogram, each 10 second fluorescence intensity trace (as in figure 2a) was broken down into one million 10μs intervals or bins (PCH bin time = 10μs). Histograms were constructed in which the number of 10μs bins is plotted on the y-axis and photon counts on the x-axis. The resulting histogram depicts the number of bins that registered 1,2,3…n photon counts during one 10 second observation period.

Photon counting histograms for biogenic amine GPCR and dimeric CD-28 (figure 3) show an average number of photon counts per 10μs bin time of 1.25, equivalent to 125,000 counts per second. Dividing by the average number of molecules calculated from the amplitude of the autocorrelation curves in figure 2b (using equation 3 with a 3D PCH model where N=7) yields an average molecular brightness of 17,857 CPSM for the GPCR and dimeric CD-28. For the β_2-AR BiFC pair, the PCH predicts 0.4 photon counts

Molecular Pharmacology Fast Forward. Published on August 1, 2013 as DOI: 10.1124/mol.113.087072
This article has not been copyedited and formatted. The final version may differ from this version.

per 10μs bin time, equivalent to 40,000 counts per second. Dividing by the average number of molecules calculated from the amplitude of the autocorrelation curve in figure 2b (using equation 3 with a 3D PCH model where N=4.3) yields an average molecular brightness of 9,302 CPSM.

FCS and PCH molecular brightness values for YFP- and GFP-tagged receptors are reported in table 1. Known monomeric (CD-86) and dimeric (CD-28) plasma membrane receptors with C-terminal GFP (CD-86/GFP and CD-86/GFP-GFP) and YFP (CD-28/YFP) were used to determine the molecular brightness of GFP and YFP monomers and dimers. Molecular brightness values for all GPCR tested were similar to one another and were similar to dimeric CD-28/YFP and tandem GFP attached to monomeric CD-86 (CD-86/GFP-GFP). The monomeric CD-86/GFP control was half the brightness of the dimeric control (figure 4) and of the GPCR.

An experimental paradigm using co-expression of fluorescence-tagged GPCR with an excess of untagged/non-fluorescent receptor was used as an additional measure of GPCR oligomer size. In this paradigm, HEK293 cells were co-transfected with GFP-tagged GPCR and a three-fold excess of untagged, non-fluorescent GPCR. These studies were performed using β_2-AR and M1-muscarinic receptors. If, for example, β_2-AR are monomeric, then co-expression of GFP-tagged β_2-AR with an excess of non-fluorescent β_2-AR would have no effect on the observed molecular brightness. However, if the receptors form homodimers, then this paradigm would produce dimers comprised of one GFP-tagged protomer and one non-fluorescent protomer. In this case the observed molecular brightness would be reduced by half. On the other hand, if the receptors are capable of forming tetramers, then co-expression with a three-fold excess of untagged receptor should reduce the molecular brightness by greater than 50%. Co-expression of β_2-AR/GFP with excess untagged β_2-AR or M_1/GFP with excess untagged M_1 receptor reduced the molecular brightness by approximately half. In contrast, co-expression of β_2-AR/GFP with untagged M_1 receptor had no effect on the molecular brightness of β_2-AR/GFP. These results are consistent with a homodimeric structure for β_2-AR and M_1-muscarinic receptors.

Bimolecular fluorescence complementation (BiFC) between the N-terminal and C-terminal halves of YFP attached to the β_2-AR was employed as an additional control.

Molecular Pharmacology Fast Forward. Published on August 1, 2013 as DOI: 10.1124/mol.113.087072
This article has not been copyedited and formatted. The final version may differ from this version.

BiFC involves the recombination of two non-fluorescent halves of a protein, such as the N-terminal half of YFP (N-YFP) and the C-terminal half of YFP (C-YFP). When two proteins (one with N-YFP and one with C-YFP) are in close proximity, N-YFP and C-YFP can recombine to reconstitute YFP fluorescence. In the present study, YFP BiFC pairs were created using the β_2-AR and A_{2a}-adenosine receptors. Co-expression of β_2-AR/N-YFP with β_2-AR/C-YFP in HEK293 cells results in fluorescence complementation and the generation of YFP fluorescence on the plasma membrane of transfected HEK293 cells (figure 5a). The specificity of the positive BiFC signal is demonstrated by reduced fluorescence following co-expression of β_2-AR/N-YFP with A_{2a}-adenosine/C-YFP (figure 5b), and restoration of fluorescence in cells co-expressing A_{2a}-adenosine/N-YFP with A_{2a}-adenosine/C-YFP (figure 5c).

Plasma membrane FCS analysis of cells co-expressing β_2-AR/N-YFP and β_2-AR/C-YFP yielded diffusion coefficients similar to those observed for the parent β_2-AR/YFP complex (table 1). If β_2-AR form homodimers, then the molecular brightness of the β_2-AR BiFC pair would be expected to be approximately half that observed for β_2-AR/YFP. FCS and PCH analyses revealed molecular brightness values for the β_2-AR BiFC pair that were approximately half that observed for β_2-AR/YFP and the dimeric CD-28/YFP control (table 1), again predicting a homodimeric structure for the β_2-AR.

Molecular brightness values equivalent to a homodimer, as reported in table 1, could be produced by a homogeneous population of homodimers or by a mixture of monomers, dimers and tetramers. Since FCS analysis would yield similar results in both cases (Meseth et al., 1999), PCH and reduced chi square analyses were used to determine the goodness of fit to both one and multi-component models (Müller et al.,2000). Reduced chi square values were close to unity when the PCH data were fit to a one component model for a homogeneous population of homodimers (table 1). Multi-component modeling of the PCH data to test for a mixture of monomers, dimers and tetramers did not provide a better fit of the data. Modeling the data using fixed monomer-dimer-tetramer ratios of 20%-70%-10% and 40%-40%-20% (ratios predicted to give an average molecular brightness equivalent to a dimer) produced reduced chi square values greater than three and 10, respectively (figures 6 and 7).

Molecular Pharmacology Fast Forward. Published on August 1, 2013 as DOI: 10.1124/mol.113.087072
This article has not been copyedited and formatted. The final version may differ from this version.

To determine the effect of agonist treatment on receptor diffusion rate and on GPCR oligomer status, transfected cells expressing GFP-tagged β_2-AR or M_1-muscarinic receptors were treated with 0.1μM isoproterenolol or carbachol, respectively, for one minute prior to FCS recording. As shown in table 2, diffusion rates and molecular brightness values were not altered following treatment with agonist, similar to our previous findings with serotonin 5-HT_{2C} receptors (Herrick-Davis et.al., 2012).

The FCS data presented in table 2 evaluate the relationship between molecular brightness and receptor expression level for β_2-AR and M_1-muscarinic receptors. The surface area of plasma membrane in the observation volume and the number of dimers per cell were calculated as described in the Methods section. There was no evidence of dimers dissociating into monomers or associating into tetramers over a 10-fold range of receptor expression level. Similar results were obtained for all GPCR tested in this study.

Discussion

The present study was preformed to shed light on the ongoing controversy related to class A GPCR oligomer size. Confocal microscopy-based FCS was chosen as the method of analysis based on its sensitivity and applicability to live cell membranes. FCS records the fluctuations in fluorescence intensity arising from individual fluorescent molecules, or in this case fluorescence-tagged GPCR, as they diffuse through the plasma membrane. Two different fluorescent probes were used to ensure that the results were not due to a unique photo-physical property of the fluorescent probe and to determine reproducibility of results. Diffusion coefficients for the biogenic amine receptors on the order of $7.5x10^{-9}$ cm^2/s are similar to previously published diffusion coefficients for class A GPCR (reviewed in Briddon and Hill, 2007). The diffusion rate of a membrane protein is related to the cubic root of the protein's mass, such that an eight-fold change in mass would be required to produce a two-fold change in the diffusion rate. In order to be resolved by FCS, the diffusion rates of two proteins must differ by a factor of 1.6 or greater (Meseth et.al., 1999). Therefore, GPCR

Molecular Pharmacology Fast Forward. Published on August 1, 2013 as DOI: 10.1124/mol.113.087072
This article has not been copyedited and formatted. The final version may differ from this version.

monomers, dimers and tetramers cannot be distinguished from one another based on their diffusion coefficients alone.

Information about a protein's oligomer size can be obtained by analyzing the amplitude of the fluorescence intensity fluctuations recorded during an FCS experiment and generating a photon counting histogram to determine the molecular brightness (Chen et.al., 1999). Since the molecular brightness is proportional to the number of fluorescent molecules traveling together within a protein complex, a GPCR monomer with a single fluorescent tag would have a molecular brightness of x, a dimer carrying two fluorescent tags would be 2x, a tetramer would be 4x and so forth. PCH analysis revealed similar molecular brightness values for all six GPCR tested. Molecular brightness values were similar to the dimeric controls and twice the monomeric controls, consistent with a dimeric structure for biogenic amine GPCR. Two additional plasma membrane controls were employed using BiFC constructs and co-expression with excess untagged/non-fluorescent receptor. In both cases, the results were consistent with a homodimeric structure for the biogenic amine GPCR examined in this study.

Previous studies designed to assess the oligomer status of biogenic amine GPCR have employed a variety of techniques including RET, FLIM, fluorescence recovery after photobleaching (FRAP), total internal reflection fluorescence (TIRF) and FCS. These methods differ in sensitivity and the population of receptors that they examine. RET and FLIM are proximity assays while TIRF and FCS have near single molecule sensitivity. TIRF, FRAP and FCS measure the mobile fraction of receptors and allow discrete regions of plasma membrane to be evaluated, where as BRET measures the entire pool of receptors. In terms of determining oligomer number, the methods described above have produced conflicting results even within the same biogenic amine receptor sub-family. For example, RET, FRAP and TIRF studies of M_1-, M_2- and M_3-muscarinic receptors have reported monomers (Hern et.al., 2010), dimers (Goin and Nathanson, 2006; Hern et.al., 2010; Patowary et.al., 2013) and tetramers (Pisterzi et.al., 2010; McMillin et.al., 2011; Patowary et.al., 2013). RET and FRAP studies of β_1-AR and β_2-AR have reported monomers (James et.al., 2006; Dorsch et.al., 2009), dimers (Mercier et.al., 2002; Dorsch et.al., 2009) and higher order oligomers (Dorsch et.al., 2009; Fung et.al., 2009). D_1- and D_2-dopamine receptors have been reported to form

Molecular Pharmacology Fast Forward. Published on August 1, 2013 as DOI: 10.1124/mol.113.087072
This article has not been copyedited and formatted. The final version may differ from this version.

homodimers and higher order oligomers assayed by RET (Guo et al. 2008) and using a nuclear translocation assay (O'Dowd et.al., 2011). RET studies of serotonin 5-HT_{1A} receptors have reported homodimers (Kobe et.al., 2008) and higher order oligomers (Ganguly et.al., 2011), while 5-HT_{2A}, 5-HT_{2C}, 5-HT_4 and 5-HT_7 appear to be predominantly dimeric (Brea et.al., 2009; Herrick-Davis et al., 2012; Pellissier et.al., 2011; Teitler and Klein, 2012). To complicate the issue further, FRAP and TIRF studies have suggested that β_1-AR and M_1-muscarinic receptors may exist in equilibrium between monomeric and dimeric states (Dorsch et al. 2009; Hern et al. 2010). In addition mixed populations of homodimers and higher order oligomers for D_1- and D_2-dopamine and M_3-muscarinic receptors have been reported (Fonseca and Lambert 2011; O'Dowd et.al., 2011; Patowary et al. 2013). Our FCS/PCH studies did not reveal the presence of tetramers or higher order oligomers of biogenic amine receptors on the plasma membrane. PCH provides an estimate of the average molecular brightness of all fluorescent species present in the sample (Müller et.al., 2000) thus if the GPCR tested in this study exist in monomer-dimer or dimer-tetramer equilibrium, then the observed molecular brightness values would be an average based on the monomer-dimer or dimer-tetramer composition of the sample. Reduced chi square analysis of a multi-component fit of the PCH data, testing for the presence of a mixture of monomers, dimers and tetramers, did not provide a better fit of the data than a one component analysis for a homogeneous population of homodimers.

Attempts to reconcile differences in GPCR oligomer status reported by the different methods used in the literature have led to the suggestion that receptor expression level may influence GPCR monomer-dimer and/or dimer-tetramer states on the plasma membrane, with low expression levels favoring monomeric forms and higher expression levels favoring association of dimers into tetramers (Hern et.al., 2010; Lambert, 2010; Patowary et.al., 2013). In the present study, we compared the molecular brightness of fluorescence-tagged GPCR over a 10-fold range of receptor expression levels. FCS analysis of the mobile fraction of plasma membrane receptors demonstrates that the homodimer configuration is maintained from 26,000 dimers/cell to 310,000 dimers/cell. As the FCS technique is best suited for studying proteins at low expression levels, we can't rule out the possibility that significantly higher expression

Molecular Pharmacology Fast Forward. Published on August 1, 2013 as DOI: 10.1124/mol.113.087072
This article has not been copyedited and formatted. The final version may differ from this version.

levels may lead to receptor clustering. It is recognized that palmitoylation promotes sequestration of GPCR into discrete microdomains (Kobe et.al., 2008; Day and Kenworthy, 2009; Woehler et.al., 2009), and that the majority of class A GPCR have at least one palmitoylation site in the C-terminus following helix 8. Receptor clustering into membrane microdomains would increase local receptor concentrations, complicating the interpretation of RET-based studies that monitor protein proximity, as positive RET is suggestive of but does not demonstrate protein-protein interaction. Further complicating the issue, stochastic RET has been reported for receptors clustered in membrane microdomains (Meyer et.al., 2006; Kobe et.al., 2008; Woehler et.al., 2009). In one study, serotonin 5-HT_{1A} receptors clustered in membrane microdomains gave RET values consistent with an oligomer number greater than 2, while non-palmitoylated mutant receptors that were excluded from microdomains gave an oligomer number of 2 (Woehler et.al., 2009). It is interesting to note that studies employing techniques with near single molecule sensitivity (TIRF and FCS) have only reported monomers or dimers, without tetramers or higher order oligomers (Hern et.al., 2010; Kasai et.al., 2011; Herrick-Davis et.al., 2012), as observed in the present study.

Studies examining the effect of ligand on GPCR oligomer status have produced differing results ranging from no effect, to dissociation or association of dimers into oligomers. FRET/FLIM studies of serotonin 5-HT_{1A} receptors (Kobe et.al., 2008) and FCS studies of 5-HT_{2C} receptors (Herrick-Davis et.al., 2012), along with FRAP studies of β_1-AR and β_2-AR (Dorsch et.al., 2009) and FRET studies of M_1- and M_2-muscarinic receptors (Goin et.al., 2006), report no effect of agonist on GPCR homodimer/oligomer status in intact cells. On the other hand, studies of 5-HT1A receptors (Ganguly et.al., 2011), β_2-AR (Fung et.al., 2009), M_3-muscarinic (Alvarez-Curto et.al., 2010), and D_1- and D_2-dopamine receptors (Guo et.al., 2008; O'Dowd et.al., 2011) suggest that these receptors form tetramers or higher order oligomers that are differentially regulated by treatment with various ligands. It is probable that the reported changes in GPCR dimer/oligomer status following ligand treatment are method, ligand and receptor dependent. In our FCS studies, treatment with isoproterenolol or carbachol did not result in β_2-AR or M_1-muscarinic homodimer dissociation or association into higher order oligomers. Since FCS measures mobile proteins, we can't exclude the possibility that

Molecular Pharmacology Fast Forward. Published on August 1, 2013 as DOI: 10.1124/mol.113.087072
This article has not been copyedited and formatted. The final version may differ from this version.

agonist binding enhances GPCR sequestration and possible clustering within membrane microdomains with reduced mobility (Day and Kenworthy, 2009). GPCR trafficking between mobile and less mobile fractions could potentially account for some of the variability obtained with different techniques that monitor different fractions or sub-populations of receptors within the plasma membrane.

In summary, the functional significance of homodimerization for class A GPCR is still a subject of great debate. It is possible that homodimerization is an essential step in protein folding required for exit from the endoplasmic reticulum (Salahpour et.al., 2004; Herrick-Davis et.al., 2006; Lopez-Gimenez et.al., 2007) as the dimer may represent the minimal functional signaling unit. In the present study, the enhanced sensitivity of FCS over proximity-based assays provides conclusive demonstration of the presence of biogenic amine homodimers, and lack of tetramers or higher order complexes, freely diffusing within the plasma membrane of living cells. The homodimer structure was not altered by receptor expression level or following agonist binding, consistent with the hypothesis that the homodimer represents the basic signaling unit.

Molecular Pharmacology Fast Forward. Published on August 1, 2013 as DOI: 10.1124/mol.113.087072
This article has not been copyedited and formatted. The final version may differ from this version.

Authorship contributions

Participated in research design: Herrick-Davis, Grinde, Cowan and Mazurkiewicz

Conducted experiments: Herrick-Davis, Grinde and Mazurkiewicz

Contributed analytic tools: Cowan

Performed data analysis: Herrick-Davis and Mazurkiewicz

Wrote or contributed to the writing of the manuscript: Herrick-Davis, Cowan, Grinde and Mazurkiewicz

References

Albizu L, Cottet M, Kralikova M, Stoev S, Seyer R, Brabet I, Roux T, Bazin H, Bourrier, E, Lamarque L, Breton C, Rives M, Newman A, Javitvh J, Trinquet E, Manning M, Pin JP, Mouillac B, and Durroux, T (2010) Time-resolved FRET between GPCR ligands reveals oligomers in native tissues. *Nat. Chem. Biol.* **6:** 587-594.

Alvarez-Curto E, Ward RJ, Pediani JD, and Milligan G (2010) Ligand regulation of the quaternary organization of cell surface M3 muscarinic acetylcholine receptors analyzed by fluorescence resonance energy transfer (FRET) imaging and homogeneous time-resolved FRET. *J. Biol. Chem.* **285:** 23318-23330.

Brea J, Castro M, Giraldo J, López-Giménez JF, Padín JF, Quintián F, Cadavid MI, Vilaró MT, Mengod G, Berg KA, Clarke WP, Vilardaga JP, Milligan G, and Loza MI (2009) Evidence for distinct antagonist-revealed functional states of 5-hydroxytryptamine(2A) receptor homodimers. *Mol Pharmacol.* **75:** 1380-1391.

Briddon SJ and Hill SJ (2007) Pharmacology under the microscope: the use of fluorescence correlation spectroscopy to determine properties of ligand-receptor complexes. *Trends Pharmacol. Sci.* **28:** 637-645.

Canals M, Burgueño J, Marcellino D, Cabello N, Canela EI, Mallol J, Agnati L, Ferré S, Bouvier M, Fuxe K, Ciruela F, Lluis C, and Franco R (2004) Homodimerization of adenosine A2A receptors: qualitative and quantitative assessment by fluorescence and bioluminescence energy transfer, *J. Neurochem.* **88:** 726-734.

Chen Y, Muller JD So PT, and Gratton E. (1999) The photon counting histogram in fluorescence fluctuation spectroscopy. *Biophysical J.* **77:** 553-567.

Chen Y, Wei L, and Muller JD (2003) Probing protein oligomerization in living cells with fluorescence fluctuation spectroscopy. *PNAS* **100:** 15492-15497.

Cole RW, Jinadasa T and Brown CM (2010) Measuring and interpreting point spread functions to determine confocal microscope resolution and ensure quality control. *Nature Protocols* **6**:1929-1941.

Day CA and Kenworthy KA (2009) Tracking microdomain dynamics in cell membranes. *Biochimica et Biophysica Acta* **1788:** 245–253.

Digman MA, Brown CM, Sengupta P, Wiseman PW, Horwitz AR, and Gratton E (2005) Measuring fast dynamics in solutions and cells with a laser scanning microscope. *Biophys. J.* **89:** 1317-1327.

Dorsch S, Klotz KN, Engelhardt S, Lohse MJ, and Bünemann M (2009) Analysis of receptor oligomerization by FRAP microscopy. *Nat. Methods.* **6:** 225-230.

Fonseca JM and Lambert NA (2009) Instability of a class a G protein-coupled receptor oligomer interface. *Mol Pharmacol.* **75:** 1296-1299.

Fotiadis D, Liang Y, Filipek S, Saperstein DA, Engel A, and Palczewski K (2003) Atomic-force microscopy: Rhodopsin dimers in native disc membranes. *Nature* **421**:127-128.

Fung JJ, Deupi X, Pardo L, Yao XY, Velez-Ruiz GA, DeVree BT, Sunahara RK, and Kobilka BK (2009) Ligand-regulated oligomerization of beta2-adrenoceptors in a model lipid bilayer. *EMBO J.* **28**: 3315–3328.

Ganguly S and Chattopadhyay A (2010) Cholesterol depletion mimics the effect of cytoskeletal destabilization on membrane dynamics of the serotonin1A receptor: A zFCS study. *Biophys J.* **99:**1397-407.

Ganguly S, Clayton AH, and Chattopadhyay A (2011) Organization of higher-order oligomers of the serotonin$_1$(A) receptor explored utilizing homo-FRET in live cells. *Biophys. J*. **100:**361-368.

Goin JC and Nathanson NM (2006) Quantitative analysis of muscarinic acetylcholine receptor homo- and heterodimerization in live cells: regulation of receptor down-regulation by heterodimerization. *J. Biol. Chem.* **281:** 5416–5425

Guo W, Urizar E, Kralikova M, Mobarec JC, Shi L, Filizola M, and Javitch JA (2008) Dopamine D2 receptors form higher order oligomers at physiological expression levels. *EMBO J.* **27:** 2293–2304.

Harikumar KG, Happs RM, and Miller LJ (2008) Dimerization in the absence of higher-order oligomerization of the G protein-coupled secretin receptor. *Biochim. Biophys. Acta.* **1778:** 2,555-2,563.

Hern JA, Baig AH, Machanov GI, Birdsall B, Corrie JET, Lazareno S, Molloy JE, and Birdsall NJM (2010) Formation and dissociation of M1 muscarinic receptor dimers seen by total internal reflection fluorescence imaging of single molecules. *PNAS* **107:** 2693-2698.

Herrick-Davis K, Grinde E, Harrigan TJ, and Mazurkiewicz JE (2005) Inhibition of serotonin 5-hydroxytryptamine2C receptor function through heterodimerization: receptor dimers bind two molecules of ligand and one G-protein. *J. Biol. Chem*. **280:** 40144-40151.

Herrick-Davis K, Weaver B, Grinde E, and Mazurkiewicz JE (2006) Serotonin 5-HT$_{2C}$ receptor homodimer biogenesis in the endoplasmic reticulum: Real-time visualization with confocal fluorescence resonance energy transfer. *J. Biol. Chem*. **281:** 27109-27116.

Herrick-Davis K, Grinde E, Lindsley T, Cowan A, and Mazurkiewicz JE (2012) Oligomer size of the serotonin 5-HT_{2C} receptor revealed by fluorescence correlation spectroscopy with photon counting histogram analysis: evidence for homodimers without monomers or tetramers. *J. Biol. Chem.* **287:** 23604–23614.

James JR, Oliveira MI, Carmo AM, Iaboni A, and Davis SJ (2006) A rigorous experimental framework for detecting protein oligomerization using bioluminescence resonance energy transfer. *Nat. Methods* **3**: 1001-1006.

Jastrzebska B, Ringler P, Palczewski K, and Engel A (2013) The rhodopsin-transducin complex houses two distinct rhodopsin molecules. *J. Struct. Biol.* **182**:164-172.

Kasai RS, Suzuki KGN, Prossnitz ER, Koyama-Honda I, Nakada C, Fujiwara TK, and Kusumi A (2011) Full characterization of GPCR monomer-dimer equilibrium by single molecule imaging. *J. Cell Biol.* **192:** 463-480.

Kilpatrick L, Briddon SJ, and Holliday ND (2012) Fluorescence correlation spectroscopy, combined with bimolecular fluorescence complementation, reveals the effects of β-arrestin complexes and endocytic targeting on the membrane mobility of neuropeptide Y receptors. *Biochim Biophys Acta*. **1823:**1068-1081.

Kobe F, Renner U, Woehler A, Wlodarczyk J, Papusheva E, Bao G, Zeug A, Richter DW, Neher E, and Ponimaskin E (2008) Stimulation- and palmitoylation-dependent changes in oligomeric conformation of serotonin 5-HT1A receptors. *Biochim Biophys Acta.* **1783:** 1503-1516.

Knepp AM, Periole X, Marrink SJ, Sakmar TP, and Huber T. (2012) Rhodopsin forms a dimer with cytoplasmic helix 8 contacts in native membranes. *Biochem.* **51:** 1819-1821.

Lambert NA (2010) GPCR dimers fall apart. *Sci Signal.* **3:** 12.

Liu P, Sudhaharan T, Koh RMl, Hwang LC, Ahmen S, Maruyama IN, and Wohland T (2007) Investigation of the dimerization of proteins from the epidermal growth factor receptor family by single wavelength fluorescence cross-correlation spectroscopy. *Biophysical J.* **93:**684-698.

Lopez-Gimenez JF, Canals M, Pediani JD, and Milligan G (2007) The alpha1b-adrenoceptor exists as a higher-order oligomer: effective oligomerization is required for receptor maturation, surface delivery, and function. *Mol. Pharmacol.* **71:** 1,105-1,029.

Malengo G, Andolfo A, Sidenius N, Gratton E, Zamai M, and Caiolfa VR (2008) Fluorescence correlation spectroscopy and photon counting histogram on membrane proteins. *J. Biomed. Opt.* **13:** 031215.

Magde D, Elson E, and Webb WW (1972) Thermodynamic fluctuations in a reacting system: measurement by fluorescence correlation spectroscopy. *Phys. Rev. Lett.* **29:** 705-708.

McMillin SM, Heusel M, Liu T, Costanzi S, and Wess J (2011) Structural basis of M_3 muscarinic receptor dimer/oligomer formation. *J. Biol. Chem.* **286:** 28,584-28,598.

Mercier JF, Salahpour A, Angers S, Breit A, and Bouvier M (2002) Quantitative assessment of beta 1- and beta 2-adrenergic receptor homo- and heterodimerization by bioluminescence resonance energy transfer. *J. Biol. Chem.* **277:** 44,925–44,931.

Meseth U, Wohland T, Rigler R, and Vogel H (1999) Resolution of fluorescence correlation measurements. *Biophys. J.* **76:** 1619-1631

Meyer BH, Segura JM, Martinez KL, Hovius R, George N, Johnsson K, and Vogel H. (2006) FRET imaging reveals that functional neurokinin-1 receptors are monomeric and reside in membrane microdomains of live cells. *Proc Natl Acad Sci* **103:** 2138-2143.

Milligan G (2013) The prevalence, maintenance, and relevance of G protein–coupled receptor oligomerization. *Mol pharm* **84**:158–169.

Müller JD, Chen Y, and Gratton E (2000) Resolving heterogeneity on the single molecular level with the photon-counting histogram. *Biophys. J.* **78:** 474-486.

Neugart F, Zappe A, Buk DM, Ziegler I, Steinert S, Schumacher M, Schopf E, Bessey R, Wurster K, Tietz C, Börsch M, Wrachtrup J, and Graeve L (2009) Detection of ligand-induced CNTF receptor dimers in living cells by fluorescence cross correlation spectroscopy. *Biochim. Biophys. Acta* **1788:** 1890-1900.

O'Dowd BF, Ji X, Alijaniaram M, Nguyen T, and George SR (2011) Separation and reformation of cell surface dopamine receptor oligomers visualized in cells. *Eur J Pharmacol*. **658:** 74-83.

Patel RC, Kumar U, Lamb DC, Eid JS, Rocheville M, Grant M, Rani A, Hazlett T, Patel SC, Gratton E, and Patel YC (2002) Ligand binding to somatostatin receptors induces receptor-specific oligomer formation in live cells. *PNAS* **99:** 3294-3299.

Patowary S, Alvarez-Curto E, Xu TR, Holz JD, Oliver JA, Milligan G, and Raicu V (2013) The Muscarinic M3 Acetylcholine receptor exists as two differently sized complexes at the plasma membrane. *Biochem J.* **452**:303-312.

Pellissier LP, Barthet G, Gaven F, Cassier E, Trinquet E, Pin JP, Marin P, Dumuis A, Bockaert J, Bane`res JL, and Claeysen S (2011) G Protein Activation by Serotonin Type 4 Receptor Dimers: evidence that turning on two protomers is more efficient. *J. Biol. Chem.* **286:** 9985-9997.

Pisterzi LF, Jansma DB, Georgiou J, Woodside MJ, Chou JT, Angers S, Raizu V, and Wells JW (2010) Oligomeric size of the M_2 muscarinic receptor in live cells as

determined by quantitative fluorescence resonance energy transfer. *J. Biol. Chem.* 285, **16:** 723-16,738.

Pramanik A, Olsson M, Langel Ü, Bartfai T, and Rigler R (2001) Fluorescence correlation spectroscopy detects galanin receptor diversity on insulinoma cells. *Biochem.* **40:** 10,839-10,845.

Qian H and Elson EL (1991) Analysis of confocal laser-microscope optics for 3D fluorescence correlation spectroscopy. *Appl. Opt.* **30:** 1185-1195.

Rashid AJ, So CH, Kong MM, Furtak T, El-Ghundi M, Cheng R, O'Dowd BF, and George SR (2007) D1-D2 dopamine receptor heterooligomers with unique pharmacology are coupled to rapid activation of Gq/11 in the striatum. *Proc Natl Acad Sci.* **104**: 654-659.

Rigler R, Mets U, Widengren J, and Kask P (1993) Fluorescence correlation spectroscopy with high count rate and low background: analysis of translational diffusion. *Eur. Biophys. J.* **22:** 169-175.

Saffarian S, Li Y, Elson EL, and Pike LJ (2007) Oligomerization of the EGF receptor investigated by live cell fluorescence intensity distribution analysis. *Biophysical J.* **93:** 1021-1031.

Salahpour A, Angers S, Mercier JF, Lagace M, Marillo S, and Bouvier M (2004) Homodimerization of the beta2-adrenergic receptor as a prerequisite for cell surface targeting. *J. Biol. Chem.* **279:** 33,390-33,397.

Savatier J, Jalaguier S, Ferguson ML, Cavalles V, and Royer CA (2010) Estrogen receptor interactions and dynamics monitored in live cells by fluorescence correlation spectroscopy. *Biochem.* **49:** 772-781.

Sommerhage F, Helpenstein R, Rauf A,Wrobel G, Offenhausser A, and Ingebrandt S (2008). Membrane allocation profiling: a method to characterize three-dimensional cell shape and attachment based on surface reconstruction. *Biomaterials* **29:** 3927–3935.

Teitler M and Klein MT (2012) A new approach for studying GPCR dimers: Drug-induced nactivation and reactivation to reveal GPCR dimer function in vitro, in primary culture, and in vivo*. Pharmacol. Ther.* **133:** 205-217.

Ulbrich MH and Isacoff EY (2007) Subunit counting in membrane-bound proteins. *Nature Methods* **4**:319-321.

Woehler A, Wlodarczyk J, and Ponimaskin EG (2009) Specific oligomerization of the 5HT1A receptor in the plasma membrane. *Glycoconj J.* **26:** 749-756.

Whorton MR, Bokoch MP, Rasmussen SG, Huang B, Zare RN, Kobilka B, and Sunahara RK (2007) A monomeric G protein-coupled receptor isolated in a high-density lipoprotein particle efficiently activates its G protein. *Proc. Natl. Acad. Sci.* **104:** 7682–7687.

Zacharias DA, Violin JD, Newton AC, and Tsein RY (2002) Partitioning of lipid-modified monomeric GFPs into membrane microdomains of live cells. *Science* **296:** 913-916.

Molecular Pharmacology Fast Forward. Published on August 1, 2013 as DOI: 10.1124/mol.113.087072
This article has not been copyedited and formatted. The final version may differ from this version.

Footnotes

Funding for this work was provided by a grant from the National Institute of Mental Health [R21 MH086796] awarded to KHD.

Molecular Pharmacology Fast Forward. Published on August 1, 2013 as DOI: 10.1124/mol.113.087072
This article has not been copyedited and formatted. The final version may differ from this version.

Figure Legends

Figure 1: Confocal microscopy of transfected HEK293 cells showing plasma membrane localization of YFP-tagged proteins. A) β_2-AR/YFP; B) D_1/YFP; C) dimeric CD-28/YFP; D) the upper plasma membrane of an HEK293 cell expressing β_2-AR/YFP showing the location (marked by +) where an FCS recording was made. Red scale bar = 10μm.

Figure 2: FCS recordings from the plasma membrane of HEK293 cells expressing YFP-tagged GPCR. A) Fluorescence intensity traces for one 10 second observation period. B) Autocorrelation analysis of the fluorescence intensity traces. The red line represents the autocorrelation of the observed fluorescence signal and the green line represents the fit to a two component model. The fast component (measured in microseconds) is related to the photo-physical properties of the fluorescent probe, while the slower component (measured in milliseconds) represents the translational diffusion of fluorescence-tagged receptors in the plasma membrane. Dividing the average photon count rate (kHz) determined from the fluorescence intensity trace shown in A by the number of fluorescent molecules determined from the autocorrelation curve shown in B (calculated as in equation 3) predicts the average molecular brightness of the sample expressed as counts per second per molecule.

Figure 3: Photon counting histograms of the corresponding FCS recordings shown in figure 2. To generate the histograms, each 10 second fluorescence intensity trace (shown in figure 2A) was broken down into one million 10μs intervals or bins (PCH bin time = 10μs). The number of bins is plotted on the y-axis and photon counts on the x-axis. The resulting histogram depicts the number of bins that registered 1,2,3…n photon counts during one 10 second observation period. The residuals of the curve fit (shown in the lower panels) plot the number of bins on the y-axis and photon counts on the x-axis. The data were fit to a one component model for a single homogenous population of homodimers. The residuals of the curve fit are less than 2 standard deviations and are randomly distributed about zero, indicating that the data are a good fit for the selected model, with reduced chi square equal to unity.

Figure 4: FCS recordings from the plasma membrane of HEK293 cells expressing CD-86/GFP and CD-86/GFP-GFP. A) Fluorescence intensity traces for one 10 second

Molecular Pharmacology Fast Forward. Published on August 1, 2013 as DOI: 10.1124/mol.113.087072
This article has not been copyedited and formatted. The final version may differ from this version.

observation period. B) Autocorrelation analysis of the fluorescence intensity traces. The red line represents the autocorrelation of the observed fluorescence signal and the green line represents the fit to a two component model. The fast component (measured in microseconds) is related to the photo-physical properties of the fluorescent probe, while the slower component (measured in milliseconds) represents the translational diffusion of the fluorescence-tagged receptors in the plasma membrane. C) Photon counting histograms of the corresponding FCS recordings yield molecular brightness values of 9,693 CPSM for CD-86/GFP and 18,194 CPSM for CD-86/GFP-GFP. D) Residuals of the curve fit. The data were fit to a one component model for a single homogenous population of fluorescence-tagged receptors.

Figure 5: Bimolecular fluorescence complementation. The N- and C-terminal halves of YFP were attached to the C-terminal end of β_2-AR or A_{2a}-adenosine receptors. A) HEK293 cells co-expressing β_2-AR/N-YFP with β_2-AR/C-YFP show plasma membrane YFP fluorescence 20 hrs post-transfection (left panel). The middle panel shows the DIC image and the right panel shows the merged image. Red scale bar = 10µm. B) HEK 293 cells co-expressing β_2-AR/N-YFP and A_{2a}-adenosine/C-YFP show minimal fluorescence complementation. C) Restoration of plasma membrane fluorescence complementation in HEK293 cells co-expressing A_{2a}-adenosine/N-YFP and A_{2a}-adenosine/C-YFP.

Figure 6: Single component and multi-component analyses for HEK293 cells expressing β_2-AR/GFP, 5-HT_{2A}/YFP or D_1/YFP. PCH and residuals of the curve fit for A) a one component fit of the data for single population of fluorescence-tagged receptors; B) a mixture of monomers-dimers-tetramers in a fixed 20%-70%-10% ratio; C) a mixture of monomers-dimers-tetramers in a fixed 40%-40%-20% ratio. Reduced chi square values for the one component and the multi-component 20%-70%-10% and 40%-40%-20% ratios were 0.8, 4.7 and 18, respectively, for β_2-AR/GFP; 1.1, 4.3 and 17, respectively, for 5-HT_{2A}/YFP; and 1.0, 4.6 and 18, respectively, for D_1/YFP.

Figure 7: Single component and multi-component analyses for HEK293 cells expressing M_1/GFP, M_2/YFP or α_{1b}-AR/YFP. PCH and residuals of the curve fit for A) a one component fit of the data for single population of fluorescence-tagged receptors; B) a mixture of monomers-dimers-tetramers in a fixed 20%-70%-10% ratio; C) a mixture of monomers-dimers-tetramers in a fixed 40%-40%-20% ratio. Reduced chi square values

Molecular Pharmacology Fast Forward. Published on August 1, 2013 as DOI: 10.1124/mol.113.087072
This article has not been copyedited and formatted. The final version may differ from this version.

for the one component and the multi-component 20%-70%-10% and 40%-40%-20% ratios were 0.7, 7.0 and 23, respectively, for M_1/GFP; 1.1, 3.2 and 16, respectively, for M_2/YFP; and 1.3, 6.0 and 23, respectively, for α_{1b}-AR/YFP.

Molecular Pharmacology Fast Forward. Published on August 1, 2013 as DOI: 10.1124/mol.113.087072
This article has not been copyedited and formatted. The final version may differ from this version.

Table 1: FCS and PCH analysis of HEK293 cells expressing YFP- and GFP-tagged biogenic amine receptors. Known monomeric (CD-86) and dimeric (CD-28) receptors are included as controls. M1/GFP and β2-AR/GFP were co-expressed with a three-fold excess of untagged/non-fluorescent receptor (eg. M1/GFP + M1/no tag 1:3). FCS τ_{D2} values for GPCR diffusion within the plasma membrane are reported in milliseconds (ms) and represent the average dwell time of the receptor in the observation volume. Diffusion coefficients ($\mu m^2/s$) were calculated using equation 2 (in Methods). 2D FCS molecular brightness values were determined by dividing the photon count rate by the number of molecules (as in equations 3 and 4 in Methods). 3D PCH analysis was performed using the PCH module in the Zeiss Aim 4.2 software package by fitting the data to a one component model (for a single population of fluorescent species) and the resulting reduced chi square values are reported. Data represent the mean+/-sem for the number of cells (N) as indicated.

Fluorescent Receptors	Diffusion		Molecular Brightness		Reduced chi square	N
	ms	$\mu m^2/s$	2D FCS	3D PCH		
Dimeric CD-28/YFP	29.1+/-1.7	0.77+/-0.03	12,728+/-372	17,819+/-484	1.07+/-0.08	20
5-HT2A/YFP	31.1+/-0.6	0.72+/-0.01	12,714+/-255	17,927+/-332	1.13+/-0.04	25
α1b-AR/YFP	32.5+/-0.6	0.69+/-0.02	12,560+/-606	17,709+/-849	1.37+/-0.13	15
D1/YFP	30.8+/-0.6	0.73+/-0.01	12,716+/-509	17,930+/-712	1.07+/-0.04	15
M2/YFP	30.1+/-0.5	0.75+/-0.01	13,295+/-410	18,480+/-578	1.06+/-0.07	10
β2-AR/YFP	30.3+/-1.4	0.74+/-0.03	13,201+/-866	18,279+/-1311	1.11+/-0.10	12
β2-AR/YFP BiFC	31.3+/-1.1	0.72+/-0.02	6,854+/-343	9,596+/-480	1.10+/-0.06	13
Monomeric CD-86/GFP	32.7+/-1.4	0.69+/-0.03	7,088+/-135	9,364+/-390	1.04+/-0.10	12
CD-86/GFP-GFP	32.5+/-1.1	0.69+/-0.02	13,131+/-450	18,777+/-565	1.19+/-0.08	10
M1/GFP	33.7+/-2.1	0.67+/-0.04	12,594+/-295	17,852+/-410	1.04+/-0.06	20
M1/GFP + Carbachol	36.0+/-2.0	0.63+/-0.04	12,878+/-390	18,029+/-546	1.12+/-0.08	10
M1/GFP + M1/no tag (1:3)	36.5+/-0.9	0.62+/-0.02	6,980+/-334	9,912+/-434	1.08+/-0.08	10
β2-AR/GFP	32.1+/-1.0	0.70+/-0.02	12,558+/-572	18,117+/790	1.23+/-0.05	15
β2-AR/GFP + Isoproterenol	37.8+/-1.7	0.60+/-0.03	12,681+/-564	17,602+/-369	1.12+/-0.09	12
β2-AR/GFP + β2-AR/no tag (1:3)	32.0+/-1.1	0.70+/-0.02	7,087+/-216	10,564+/-300	1.05+/-0.05	13
β2-AR/GFP + M1/no tag (1:3)	35.2+/-1.7	0.63+/-0.03	12,506+/-227	17,950+/-351	1.11+/-0.09	10

Molecular Pharmacology Fast Forward. Published on August 1, 2013 as DOI: 10.1124/mol.113.087072
This article has not been copyedited and formatted. The final version may differ from this version.

Table 2: Relationship between molecular brightness and receptor expression level. Plasma membrane 2D FCS molecular brightness analysis of HEK293 cells expressing different levels of GFP-tagged M_1-muscarinic receptors (M1/GFP), β_2-adrenergic receptors (β2-AR/GFP), and monomeric CD-86 labeled with two GFP tags (CD-86/GFP-GFP). The photon count rate (kHz) is a measure of the overall fluorescence intensity of the region of plasma membrane in the observation volume and N is the number of receptor dimers in the observation volume (calculated as in equation 3). Molecular brightness values are reported as photon counts per molecule. Data represent the mean +/- sem from 3 cells with similar photon count rates (kHz). The area of plasma membrane in the observation volume was calculated using $\pi\omega_0^2$, where ω_0 is the radius of the observation volume (calculated as in Methods), and was used to determine the number of dimers per μm^2 of plasma membrane. An HEK293 cell total surface area equivalent to $2591\mu m^2$ (Sommerhage et.al., 2008) was used to estimate the total number of dimers per cell.

Receptor	Count Rate (kHz)	N	Molecular Brightness	Dimers/μm^2	Dimers/Cell
M1/GFP	37+/-1.7	3.0+/0.2	12,525+/-244	10	$2.6x10^4$
β2-AR/GFP	46+/-4.4	3.5+/-0.5	13,083+/-941	12	$3.1x10^4$
CD-86/GFP-GFP	69+/-12	5.6+/-1.2	12,537+/-595	20	$5.2x10^4$
M1/GFP	113+/-2.9	8.9+/-0.4	12,797+/-446	31	$8.0x10^4$
β2-AR/GFP	192+/-8.8	15+/-0.4	12,579+/-465	53	$1.4x10^5$
M1/GFP	206+/-7.4	16+/-0.2	12,460+/-704	56	$1.5x10^5$
CD-86/GFP-GFP	223+/-12	18+/-0.7	12,750+/-233	63	$1.6x10^5$
β2-AR/GFP	311+/-26	26+/-2.7	12,137+/-324	91	$2.4x10^5$
M1/GFP	358+/-4.5	29+/-1.2	12,496+/-707	102	$2.6x10^5$
β2-AR/GFP	413+/-19	34+/-1.0	11,970+/-285	119	$3.1x10^5$

Figure 1

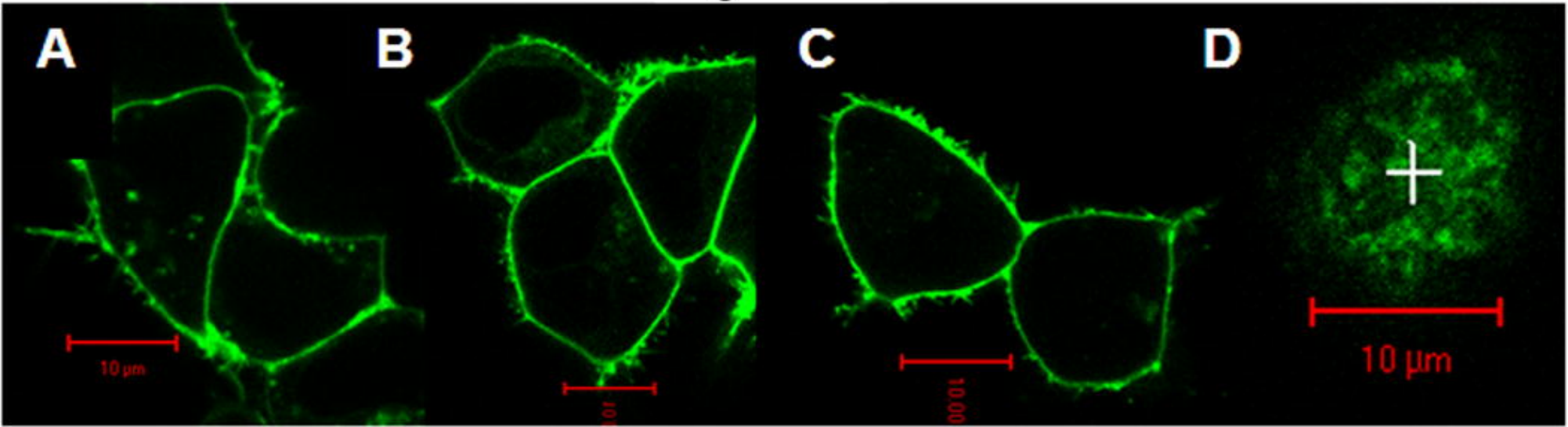

Figure 2

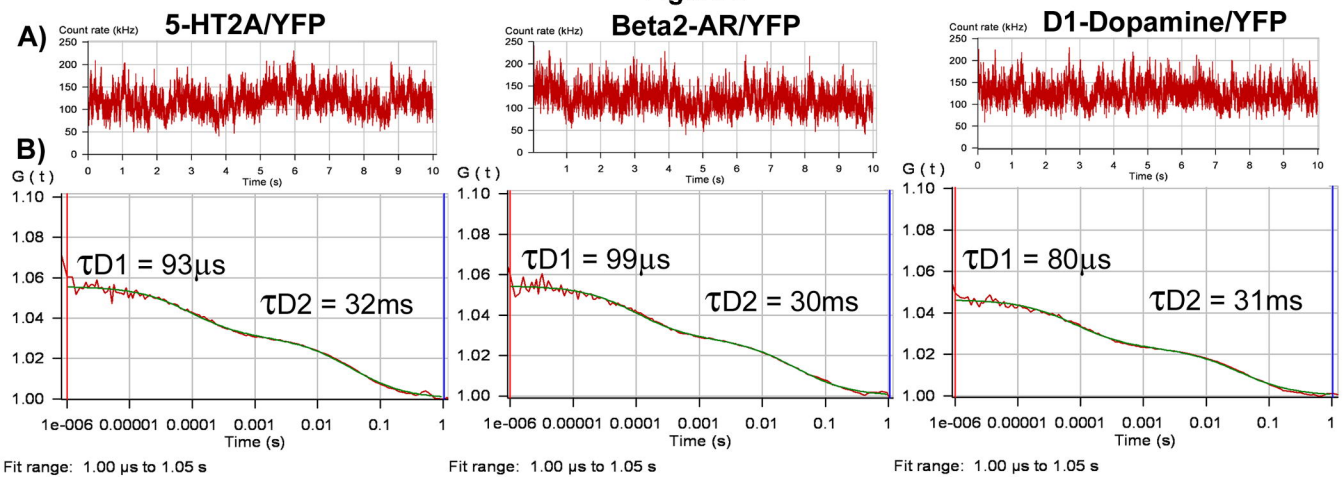
A)
5-HT2A/YFP
Beta2-AR/YFP
D1-Dopamine/YFP
Count rate (kHz)
Time (s)
B)
G (t)
τD1 = 93µs
τD2 = 32ms
τD1 = 99µs
τD2 = 30ms
τD1 = 80µs
τD2 = 31ms
Time (s)
Fit range: 1.00 µs to 1.05 s
Fit range: 1.00 µs to 1.05 s
Fit range: 1.00 µs to 1.05 s

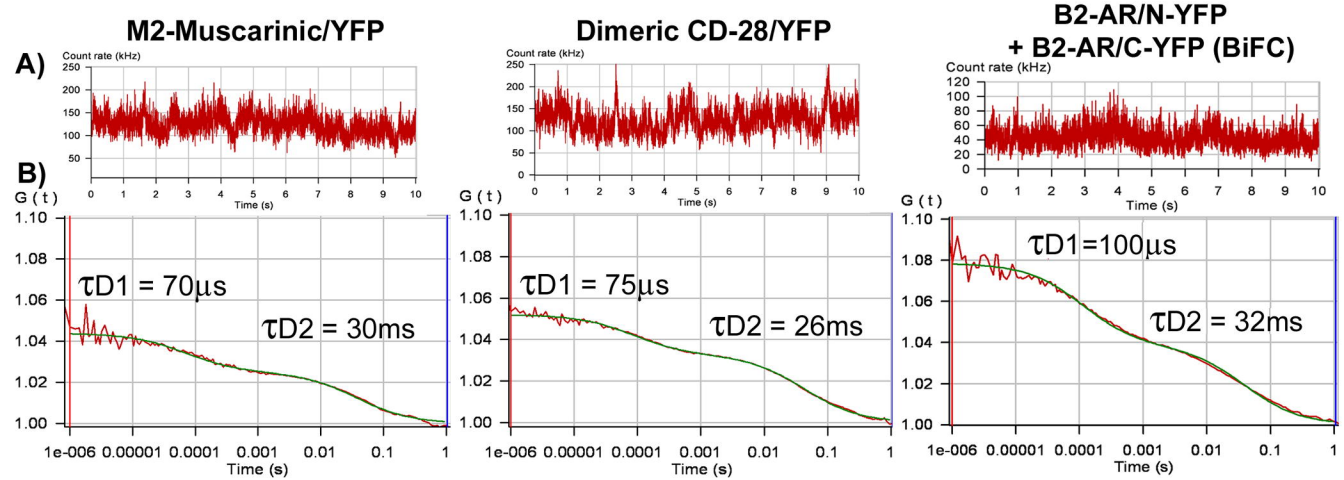
M2-Muscarinic/YFP
Dimeric CD-28/YFP
B2-AR/N-YFP
+ B2-AR/C-YFP (BiFC)
A)
Count rate (kHz)
Time (s)
B)
G (t)
τD1 = 70µs
τD2 = 30ms
τD1 = 75µs
τD2 = 26ms
τD1=100µs
τD2 = 32ms
Time (s)
Fit range: 1.00 µs to 1.05 s
Fit range: 1.00 µs to 1.05 s
Fit range: 1.00 µs to 1.05 s

Figure 3

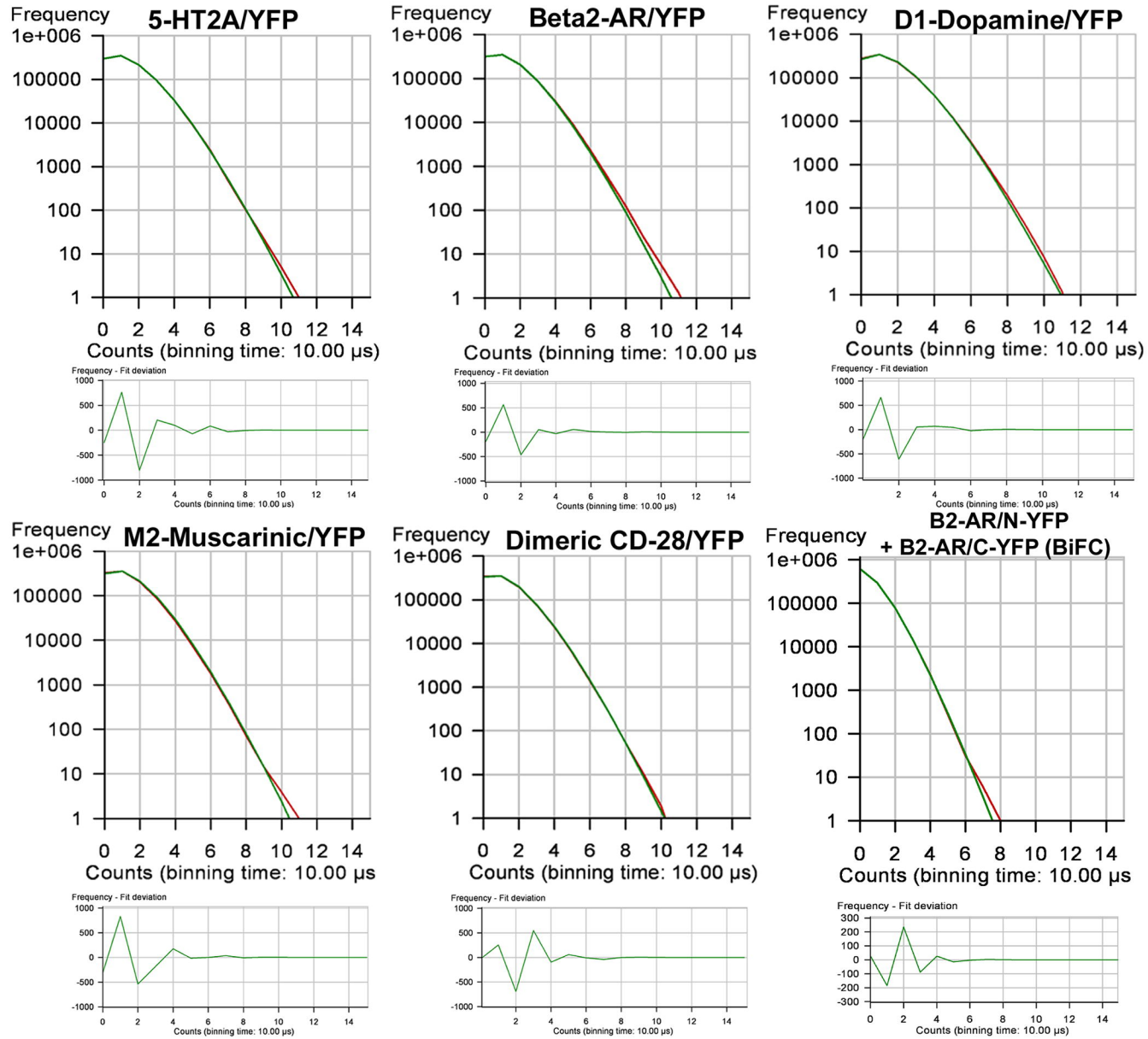
5-HT2A/YFP
Beta2-AR/YFP
D1-Dopamine/YFP
M2-Muscarinic/YFP
Dimeric CD-28/YFP
B2-AR/N-YFP
+ B2-AR/C-YFP (BiFC)
Frequency
Counts (binning time: 10.00 µs)
Frequency - Fit deviation

Figure 4

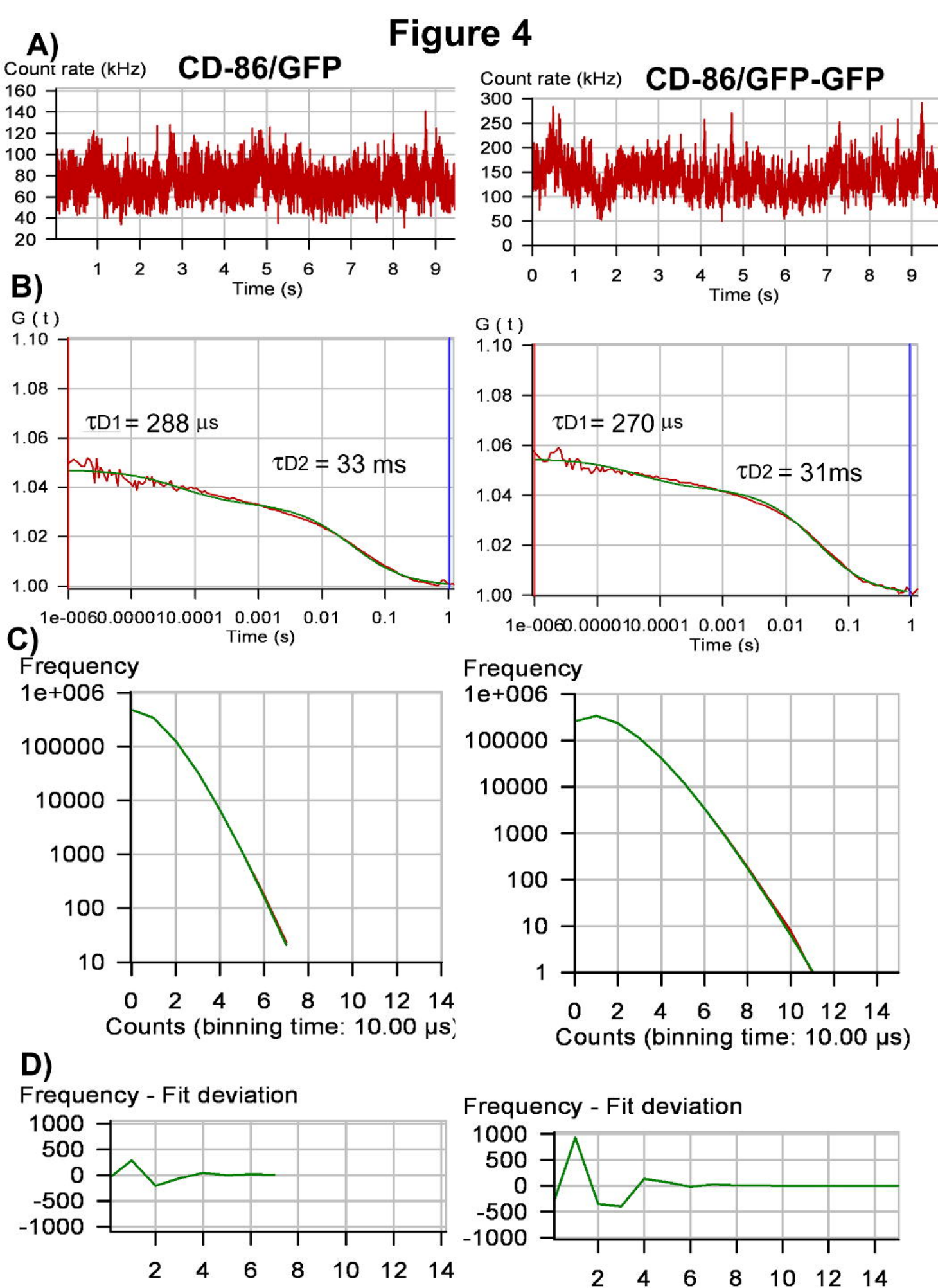
A)
Count rate (kHz)
CD-86/GFP
160
140
120
100
80
60
40
20
1 2 3 4 5 6 7 8 9
Time (s)
Count rate (kHz)
CD-86/GFP-GFP
300
250
200
150
100
50
0
0 1 2 3 4 5 6 7 8 9
Time (s)
B)
G (t)
1.10
1.08
1.06
1.04
1.02
1.00
τD1 = 288 µs
τD2 = 33 ms
1e-006 0.00001 0.0001 0.001 0.01 0.1 1
Time (s)
G (t)
1.10
1.08
1.06
1.04
1.02
1.00
τD1 = 270 µs
τD2 = 31ms
1e-006 0.00001 0.0001 0.001 0.01 0.1 1
Time (s)
C)
Frequency
1e+006
100000
10000
1000
100
10
0 2 4 6 8 10 12 14
Counts (binning time: 10.00 µs)
Frequency
1e+006
100000
10000
1000
100
10
1
0 2 4 6 8 10 12 14
Counts (binning time: 10.00 µs)
D)
Frequency - Fit deviation
1000
500
0
-500
-1000
2 4 6 8 10 12 14
Frequency - Fit deviation
1000
500
0
-500
-1000
2 4 6 8 10 12 14

Figure 5

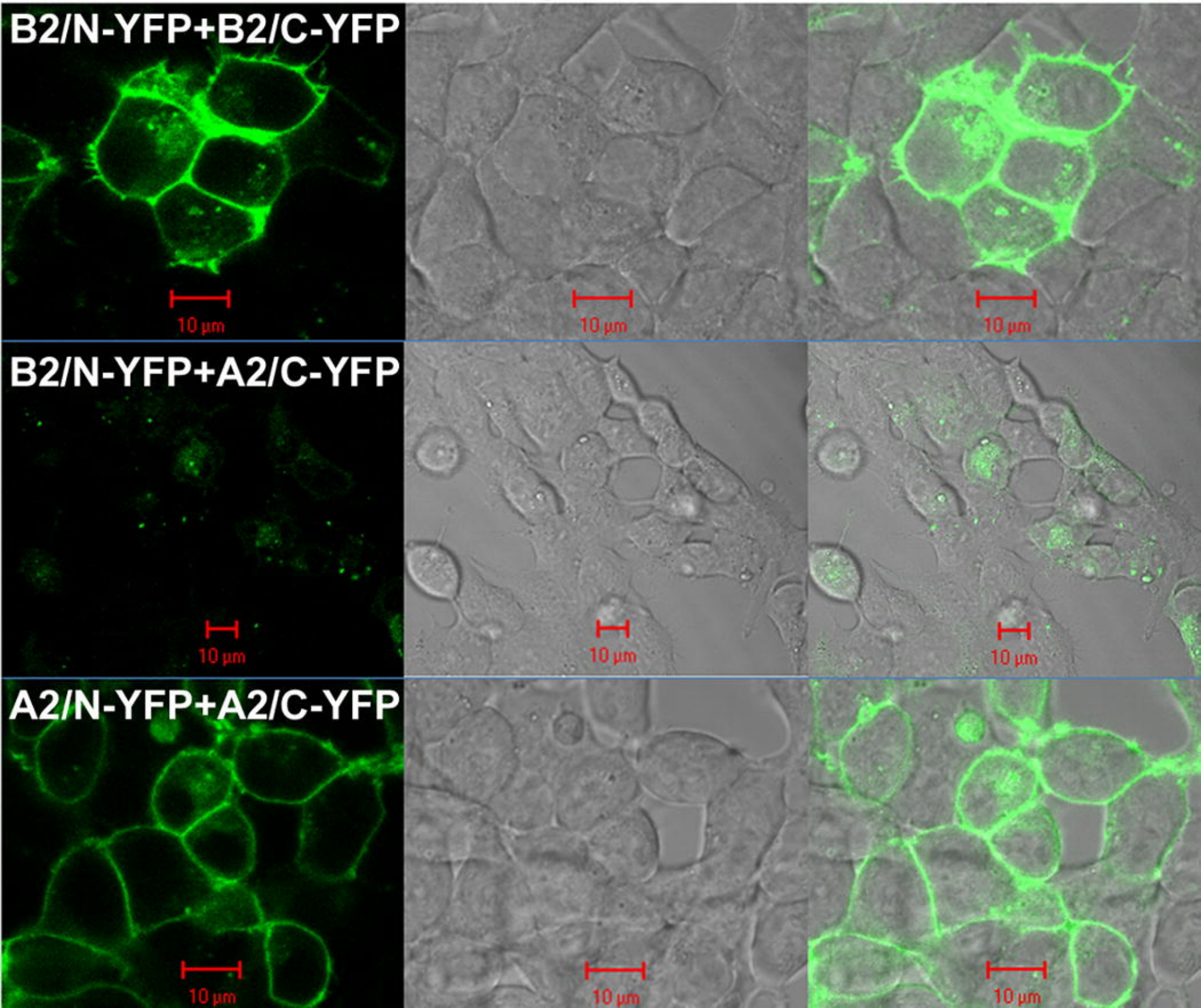
B2/N-YFP+B2/C-YFP
10 µm
10 µm
10 µm
B2/N-YFP+A2/C-YFP
10 µm
10 µm
10 µm
A2/N-YFP+A2/C-YFP
10 µm
10 µm
10 µm

Figure 6

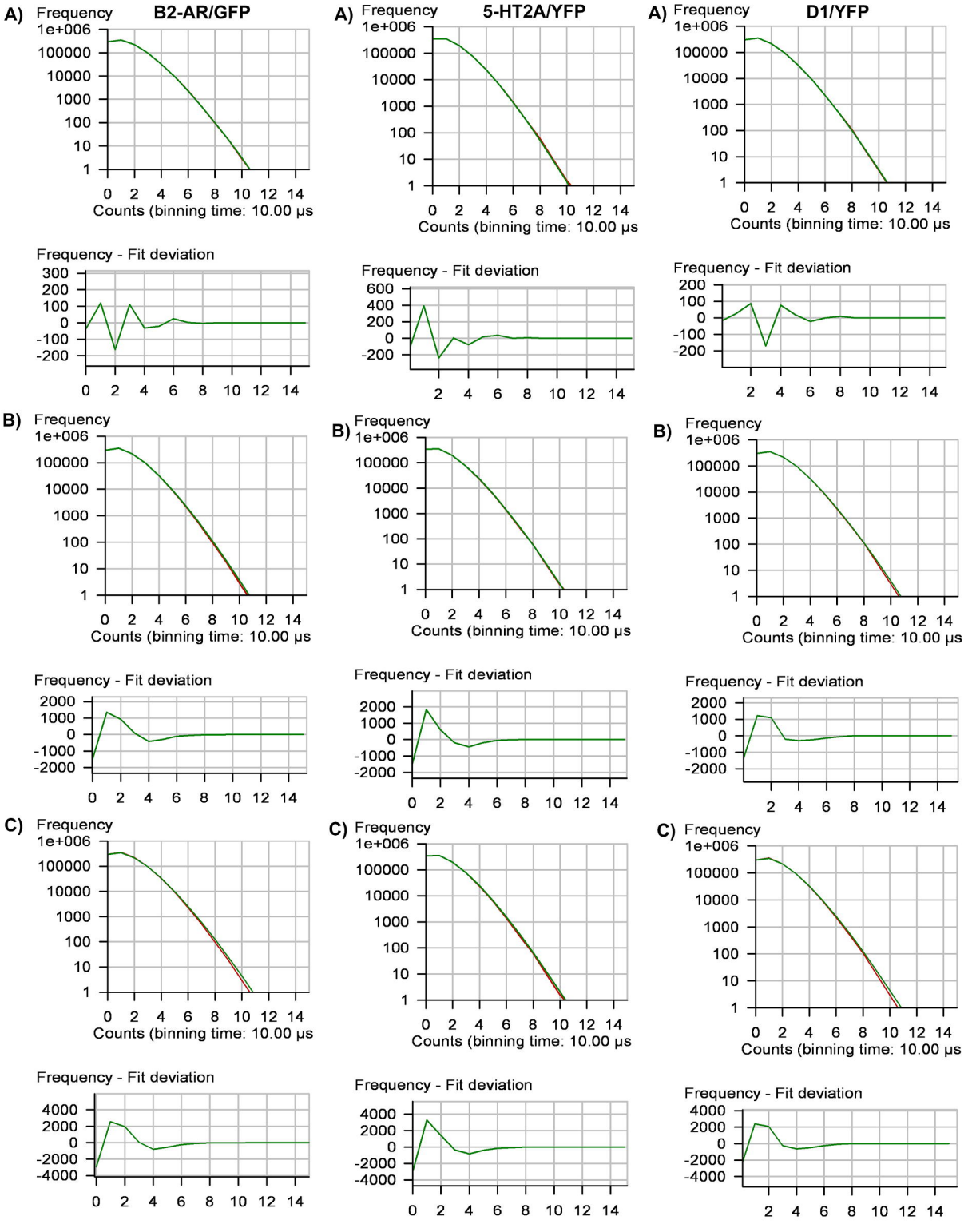
A)
B2-AR/GFP
5-HT2A/YFP
D1/YFP
Frequency
Counts (binning time: 10.00 µs
Frequency - Fit deviation
B)
C)

Figure 7

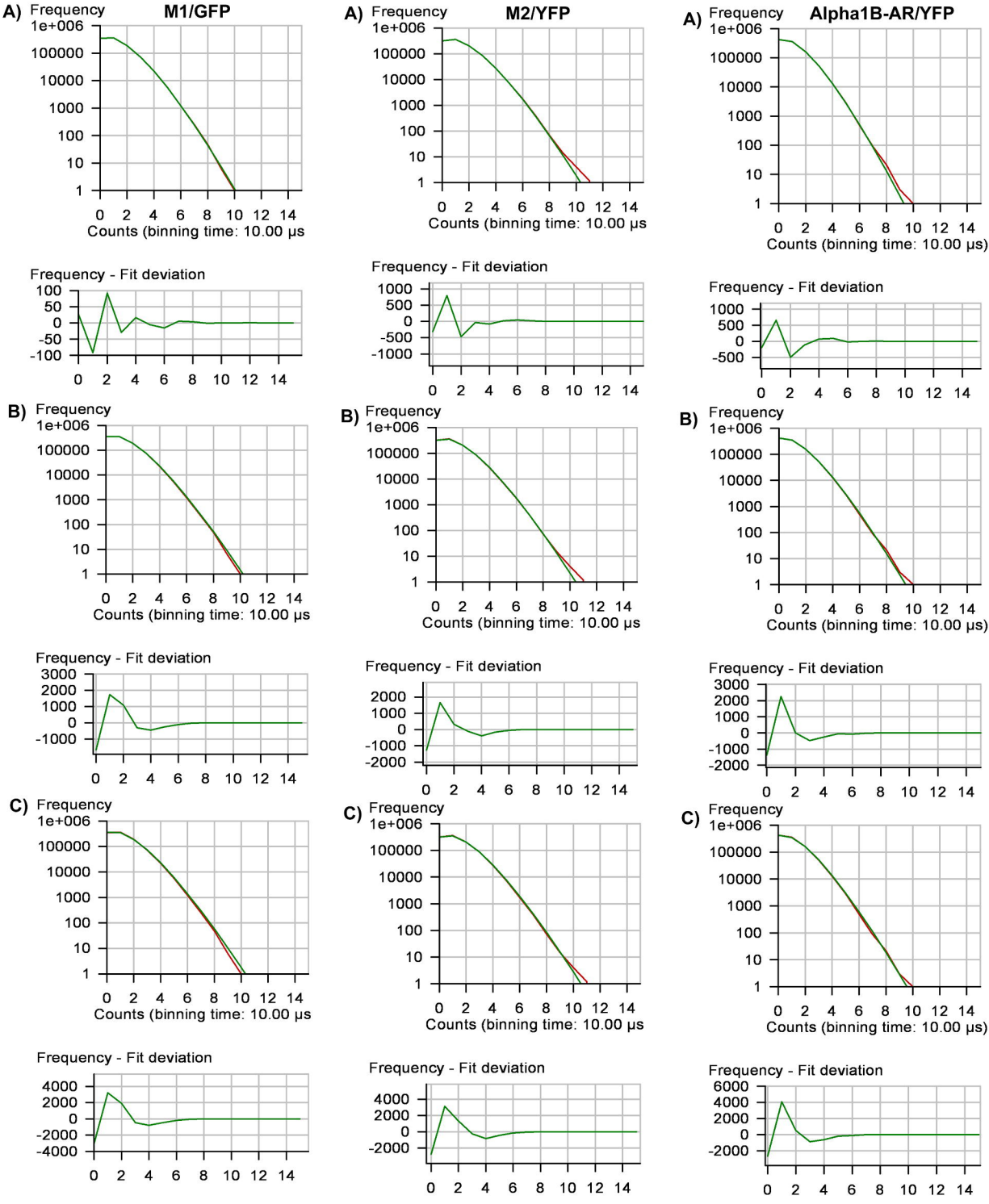
A)
Frequency
M1/GFP
1e+006
100000
10000
1000
100
10
1
0 2 4 6 8 10 12 14
Counts (binning time: 10.00 µs
Frequency - Fit deviation
100
50
0
-50
-100
0 2 4 6 8 10 12 14
B)
Frequency
1e+006
100000
10000
1000
100
10
1
0 2 4 6 8 10 12 14
Counts (binning time: 10.00 µs
Frequency - Fit deviation
3000
2000
1000
0
-1000
0 2 4 6 8 10 12 14
C)
Frequency
1e+006
100000
10000
1000
100
10
1
0 2 4 6 8 10 12 14
Counts (binning time: 10.00 µs
Frequency - Fit deviation
4000
2000
0
-2000
-4000
0 2 4 6 8 10 12 14
A)
Frequency
M2/YFP
1e+006
100000
10000
1000
100
10
1
0 2 4 6 8 10 12 14
Counts (binning time: 10.00 µs
Frequency - Fit deviation
1000
500
0
-500
-1000
0 2 4 6 8 10 12 14
B)
Frequency
1e+006
100000
10000
1000
100
10
1
0 2 4 6 8 10 12 14
Counts (binning time: 10.00 µs
Frequency - Fit deviation
2000
1000
0
-1000
-2000
0 2 4 6 8 10 12 14
C)
Frequency
1e+006
100000
10000
1000
100
10
1
0 2 4 6 8 10 12 14
Counts (binning time: 10.00 µs
Frequency - Fit deviation
4000
2000
0
-2000
0 2 4 6 8 10 12 14
A)
Frequency
Alpha1B-AR/YFP
1e+006
100000
10000
1000
100
10
1
0 2 4 6 8 10 12 14
Counts (binning time: 10.00 µs)
Frequency - Fit deviation
1000
500
0
-500
0 2 4 6 8 10 12 14
B)
Frequency
1e+006
100000
10000
1000
100
10
1
0 2 4 6 8 10 12 14
Counts (binning time: 10.00 µs)
Frequency - Fit deviation
3000
2000
1000
0
-1000
-2000
0 2 4 6 8 10 12 14
C)
Frequency
1e+006
100000
10000
1000
100
10
1
0 2 4 6 8 10 12 14
Counts (binning time: 10.00 µs)
Frequency - Fit deviation
6000
4000
2000
0
-2000
0 2 4 6 8 10 12 14